Available online at www.sciencedirect.com
SCIENCE DIRECT®
Polymer Degradation and Stability 91 (2006) 1025–1035
Polymer Degradation and Stability
www.elsevier.com/locate/polydegstab

Influence of isocyanate type of acrylated urethane oligomer and of additives on weathering of UV-cured films

Byoung-Hoo Lee, Hyun-Joong Kim*

Laboratory of Adhesion and Bio-Composites, Major in Environmental Materials Science, Seoul National University, Seoul 151-921, South Korea

Received 19 April 2005; received in revised form 28 July 2005; accepted 2 August 2005
Available online 24 October 2005

Abstract

The weathering of UV-cured films containing the isocyanate type of acrylated urethane oligomer, and the influence of different additives (HALS, UVA and TiO_2), was investigated by various methods. The UV-cured film containing the acrylated aromatic urethane oligomer showed worse photodegradation than that containing the acrylated aliphatic urethane oligomer. In the case of the UV-cured films containing the acrylated aromatic urethane oligomer, those stabilized using both HALS and UVA showed the highest photostability.

Keywords: UV-curable urethane acrylate coating; Acrylated urethane oligomer; HALS; UVA; Weathering; Photodegradation

1. Introduction

The technology of UV curing is based on coating components, which consist of an oligomer, a monomer and a photoinitiator. All of these components can be cured under UV light.

The most commonly used UV-curable formulations contain unsaturated acrylates. The main types of acrylic oligomers are epoxy acrylates, polyester acrylates, polyether acrylates, urethane acrylates and silicone acrylates. Among the oligomers used for UV-curable coatings, urethane acrylate oligomers offer a wide range of excellent application properties, such as high impact and tensile strength, abrasion resistance and toughness combined with excellent resistance to chemicals and solvents. Coatings with suitable flexibility, good adhesion to difficult substrates and excellent weathering resistance can be obtained by using a suitable selection of aromatic or aliphatic urethane acrylates. In terms of the durability of the coatings, aromatic systems are disadvantageous, since they have a stronger tendency to yellow and degrade photochemically, due to their stronger absorption of light in the ultraviolet region. Thus, aliphatic systems are employed in highly durable applications, because of their high photochemical resistance [1]. UV-curable coatings have found a large number of applications in various products such as a wood, paper and paperboard, plastics, metal, glass and ceramics, as well as other miscellaneous applications [1].

Recently, the use of UV-curable coatings has been seriously considered by the automobile industry for body coating applications [2]. In particular, since the UV-curable coatings used for outdoor products are continuously subjected to weathering and other environmental factors throughout their service life, it is important to understand the weathering-induced degradation of the cured film [3].

During their outdoor exposure, polymers degrade chemically and mechanically, due to the combined action of sunlight (especially the short wavelength UV rays present in the solar spectrum), oxygen, moisture, and heat [4,5]. The service life of the coating film in outdoor applications is limited due to this weathering effect.

Scientists have tried to understand why and how the degradation of the coating film occurs [6,7]. In addition, to enhance the durability of the cured film, stabilizer additives such as hindered amine light stabilizers (HALSs), ultraviolet light absorbers (UVAs) or combinations of the two are added to the coating formulation [7].

* Corresponding author. Tel.: +82 2 880 4784; fax: +82 2 873 2318.
E-mail address: hjokim@snu.ac.kr (H.-J. Kim).

0141-3910/$ - see front matter © 2005 Elsevier Ltd. All rights reserved.
doi:10.1016/j.polymdegradstab.2005.08.002

Table 1
Characteristics of the oligomers

Oligomers	Viscosity[c] (mPa.s)	Density (g/cm^3)	Molecular weight	Functionality	Polymer solids (wt.%)	T_g (°C)
Ebecryl® 210[a]	3900	1.11	1500	2	100	−19
Ebecryl® 270[b]	3000	1.10	1500	2	>95	−32

[a] Aromatic urethane diacrylate oligomer.
[b] Aliphatic urethane diacrylate oligomer.
[c] Höppler viscosity at 60 °C.

However, because UV-curable coatings have not been extensively used in outdoor environments, their long-term weathering behaviours are largely unknown [2]. Therefore, the purpose of this study was to evaluate the influence of the isocyanate type of acrylated urethane oligomer, and that of the additives used, on the weathering properties of UV-cured urethane acrylate films.

2. Experimental

2.1. Materials

The UV-curable urethane acrylate system consisted of four main components: firstly, aliphatic urethane diacrylate (Ebecryl®270, UCB) oligomer or/and aliphatic urethane diacrylate (Ebecryl®210, UCB) oligomer (Table 1); secondly, a reactive diluent monomer; and thirdly, the photoinitiators used to obtain the UV-curable coatings. Finally, additives were used to improve the photodegradation resistance. The reactive diluent monomer was 1,6-hexanediol diacrylate (Miramer M200, Miwon).

Two different photoinitiators were used. These were 1-hydroxy-cyclohexyl-phenyl ketone (Micure CP-4, Miwon), and bis(2,4,6-trimethylbenzoyl)-phenylphosphine oxide (Irgacure®819, Ciba Specialty Chemicals). In addition, the UV-curable coatings were stabilized using Tinuvin 384-2 (95% benzenepropanoic acid, 3-(2H-benzotriazol-2-yl)-5-(1,1-dimethylethyl)-4-hydroxy-, C7–9-branched and linear alkyl esters, 5% 1-methoxy-2-propyl acetate; UVA) and/or Tinuvin 292 (mixture of bis(1,2,2,6,6-pentamethyl-4-piperidinyl)-sebacate and 1-(methyl)-8-(1,2,2,6,6-pentamethyl-4-piperidinyl)-sebacate; HALS).

The light stabilizers are shown in Fig. 1. As shown in Fig. 2, the bis-phenylphosphine oxide photoinitiator absorbs longer wavelength light than the light stabilizer (UVA). This demonstrates that the bis-phenylphosphine oxide photoinitiator having sufficient absorption at a wavelength greater than the absorption wavelength of the light stabilizer is suitable for the curing of the UV-curable coating system, which is stabilized using the light stabilizer.

In addition, we added TiO_2 to the UV-curable coating in the case of the pigmented system. The UV-curable coatings were formulated as shown in Table 2. The viscosities of the prepared UV-curable coatings were measured by means of a Programmable Viscometer Model DV-α+ at 25 °C, using an RV 4 spindle. Table 3 shows the viscosities of the prepared UV-curable coatings.

2.2. Process of UV curing

In order to investigate the change in the discoloration, gloss and hardness of the cured film during the accelerated weathering, each UV-curable coating was coated onto a white tile (15 cm × 6 cm × 1 cm) using a bar coater (No. 22) and cured in a conveyer belt type UV curing machine equipped with a high-pressure mercury lamp (100 W/cm, main wavelength: 365 nm).

The surface of the white tile was cleaned with acetone and air-dried prior to the application. For heat-sensitive applications, a cold mirror was used as a reflector. The UV dose used was 1360 mJ/cm^2. The thickness of the cured film was 40 μm.

In addition, in order to investigate the change in the morphology and chemical structure of the cured film during the accelerated weathering, each UV-curable coating was coated onto thin aluminium foil (15 cm × 6 cm × 19 μm) using a bar coater. These samples were cured using the same procedure as that described above. After each accelerated weathering test, the samples were carefully cut into test samples of a suitable size, in order to measure their photochemical degradation.

2.3. Accelerated weathering test

To evaluate the resistance of the UV-cured film to photochemical degradation, the test samples were placed in a

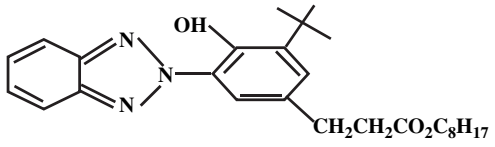

95% benzenepropanoic acid, 3-(2H-benzotriazol-2-yl)-5-(1,1-dimethylethyl)-4-hydroxy-, C7-9-branched and linear alkyl esters, 5% 1-methoxy-2-propyl acetate (Tinuvin 384-2)

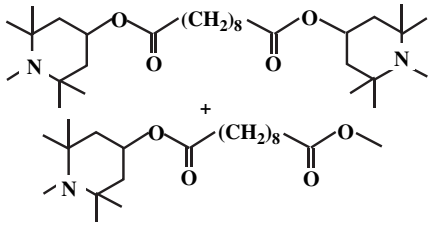

Mixture of bis (1,2,2,6,6-pentamethyl-4-piperidinyl) sebacate and 1-(methyl)-8-(1,2,2,6,6-pentamethyl-4-piperidinyl) sebacate (Tinuvin 292)

Fig. 1. Light stabilizers.

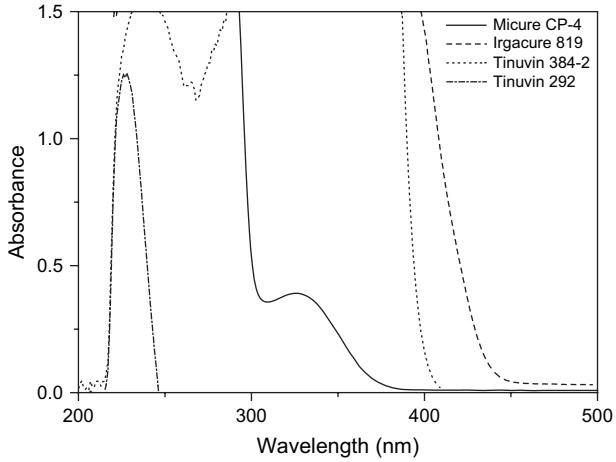

Fig. 2. Absorption spectra of the photoinitiators and light stabilizers (0.1% in acetonitrile).

Q-SUN Xenon Test Chamber (Q-SUN/1000, Q-Panel Lab Products, USA) equipped with a Xenon arc lamp. The irradiation setting was 0.68 W/m^2 at 420 nm. The Q-SUN Xenon Test Chamber was operated under the light condition. The black panel temperature in the test chamber was 60 °C. The test samples were exposed for up to 960 h and removed at regular intervals to observe the extent of the photodegradation of the cured film.

2.4. Analysis

2.4.1. Discoloration measurement

During the accelerated weathering, the surface colour difference of the test samples was measured in order to record the photochemical degradation.

The surface colour difference (ΔE^*) was measured using a Brightimeter Micro S-5 (Technidyne Co., USA). The surface colour difference was calculated using the CIE $L^*a^*b^*$ system.

$$\Delta L^* = L_f^* - L_i^*$$

$$\Delta a^* = a_f^* - a_i^*$$

$$\Delta b^* = b_f^* - b_i^*$$

where L^*, a^*, and b^* represent the lightness, yellowness, and redness, respectively.

$$\Delta E^* = \left(\Delta L^{*2} + \Delta b^{*2} + \Delta a^{*2}\right)^{1/2}$$

where ΔL^*, Δa^*, and Δb^* represent the changes between the initial (i) and current (f) values.

2.4.2. Gloss measurement

The surface gloss retention (%) of the cured films at an angle of incidence/reflection of 20° was measured by a Tri-Microgloss (Sheen, England).

$$\text{Gloss retention}\ (\%) = \left(G_f/G_i\right) \times 100$$

where G_i and G_f represent the initial and current gloss values, respectively.

2.4.3. Pendulum hardness test

A König pendulum hardness tester (Ref. 707PK, Sheen Instruments Ltd, England) was used to monitor the surface hardness of the cured film during the accelerated weathering [8].

Table 2
Formulations of the UV-curable coatings

Components		Compositions (wt.%)						
		Al	Al/Ar	Ar	ArU	ArH	ArUH	ArP
Oligomers	Ebecryl 210[a]		23.5	57	55.2	55.2	55.2	45
	Ebecryl 270[b]	57	23.5					
Monomer	Miramer M200[c]	38	38	38	36.8	36.8	36.8	30
Photoinitiators	Micure CP-4[d]	5	5	5	3	3	3	3
	Irgacure 819[e]				2	2	2	2
Light stabilizers	Tinuvin 384-2[f]				3		2	
	Tinuvin 292[g]					3	1	
Pigment	Dupont R706[h]							20
Total (wt.%)		100	100	100	100	100	100	100

[a] Ebecryl 210 (aromatic urethane diacrylate).
[b] Ebecryl 270 (aliphatic urethane diacrylate).
[c] Miramer M200 (1,6-hexanediol diacrylate).
[d] Micure CP-4 (1-hydroxy-cyclohexyl-phenyl-ketone).
[e] Irgacure 819 (bis(2,4,6-trimethylbenzoyl)-phenylphosphine oxide).
[f] Tinuvin 384-2 (95% benzenepropanoic acid, 3-(2H-benzotriazol-2-yl)-5-(1,1-dimethylethyl)-4-hydroxy-, C7–9-branched and linear alkyl esters, 5% 1-methoxy-2-propyl acetate (UV absorber type)).
[g] Tinuvin 292 (mixture of bis(1,2,2,6,6-pentamethyl-4-piperidinyl)-sebacate and 1-(methyl)-8-(1,2,2,6,6-pentamethyl-4-piperidinyl)-sebacate (hindered amine light stabilizer type)).
[h] Dupont R706 (titanium dioxide).

Table 3
Viscosities of the UV-curable coatings

Viscosity[a] (cP)						
Al	Al/Ar	Ar	ArU	ArH	ArUH	ArP
578	604	644	714	650	674	964

[a] Measured by programmable viscometer Model DV-α+ at 25 °C (spindle RV 4).

2.4.4. Microhardness test

During the accelerated weathering, the change in the surface hardness of the UV-cured films was characterized using a computer-controlled Fischerscope H 100 XYp microhardness tester equipped with a Vickers diamond indenter.

The plastic hardness, H, and universal hardness, HU, measured by this instrument are defined by the following formulae [9]:

$$H = L_{max}/26.43 \times (d_{corr})^2$$

$$HU = L_{max}/26.43 \times (d_{max})^2$$

where the diamond indenter maximum load, L_{max}, and the diamond indenter penetration depths, d_{corr} and d_{max}, are defined in Fig. 3. The plastic hardness, H, is determined only by the plastic component of the cured film deformation. On the other hand, the universal hardness, HU, is determined by both the plastic and elastic components of the cured film deformation [9]. In Fig. 3, the slope is defined by the tangent to the unloading curve at L_{max}.

In addition, the elastic and plastic portions of the indentation work are defined by the following formulae:

$$W_{total} = \int L \, dd \text{ (within the limits } d = 0 \text{ and } d = d_{max})$$

where W_{total} ($= W_{elast} + W_{plas}$) is the total deformation work, and W_{plas} and W_{elast} are the plastic (area 1), and elastic deformation works (area 2).

$$\text{Elastic portion of the indentation work } (\%) = W_{elast}/W_{total} \times 100$$

$$\text{Plastic portion of the indentation work } (\%) = W_{plas}/W_{total} \times 100$$

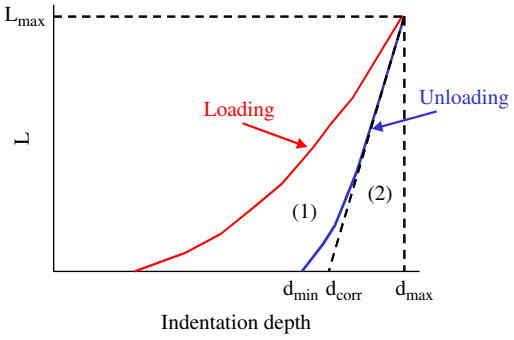

Fig. 3. Typical indentation load-displacement curve measured using a microhardness tester. Areas (1) and (2) represent the plastic deformation and elastic recovery, respectively [9].

The microhardness test was performed at a maximum load of 30 mN. The loading time was 20 s. During the loading time, the load was gradually increased until the maximum load was reached. Five hardness values were measured at different surface locations, in order to obtain reasonable statistics.

2.4.5. Fourier transformation infrared spectroscopy (FT-IR)

The IR spectra of the UV-cured films during the accelerated weathering were obtained using a Nicolet Magna 550 Series II FT-IR spectroscope (Midac Co., USA) equipped with attenuated total reflectance (ATR). The ATR crystal was of zinc selenide (ZnSe). The resolution of the spectra recorded was 4 cm^{-1}. In order to obtain the IR spectra of the UV-cured films during the accelerated weathering, the ZnSe crystal was covered with the coated thin aluminium foil, which was removed at regular time intervals from the accelerated weathering chamber.

In the case of the UV-cured films containing the acrylated aromatic oligomer, in order to monitor the photochemical degradation of the UV-cured film, the peak corresponding to the C–N stretch at around 1529 cm^{-1}, which is related to the urethane linkage, and the peak corresponding to the C–H stretch at around 2931 cm^{-1} were chosen [10]. In the case of the UV-cured films containing the acrylated aliphatic oligomer, the peak corresponding to the C–N stretch at around 1533 cm^{-1} and the peak corresponding to the C–H stretch at around 2931 cm^{-1} were chosen [6,11].

The conversion of each peak was calculated by means of the following equation:

$$\text{Conversion } (\%) = (A_0 - A_t)/A_0 \times 100$$

where A_0 is the peak area before exposure (exposure time 0) and A_t is the peak area at exposure time t.

2.4.6. Atomic force microscopy

In order to observe the changes in the surface morphology of the UV-cured films during the accelerated weathering, atomic force microscopy (AFM) was performed using a Dimension SPM-3000 instrument (Digital Instruments, USA).

A small specimen (2 cm × 2 cm) was cut from the coated aluminium foil whenever it was removed from the accelerated weathering chamber at the different exposure intervals. The surface morphology was examined by recording AFM images in tapping mode. The values of the root mean square (RMS) roughness were calculated from the height values in the AFM images using the DI software. All images were obtained in air and collected using a scan size of 20 μm.

3. Results and discussion

3.1. Discoloration

Fig. 4 shows the influence of the isocyanate type of acrylated urethane oligomer, and that of the additives (HALS, UVA and TiO_2) used, on the discoloration of the UV-cured

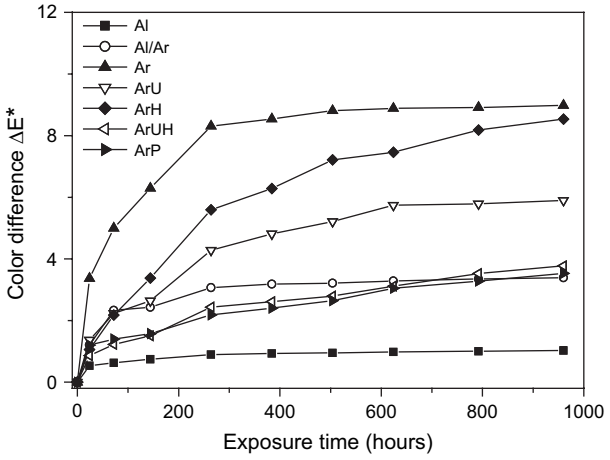

Fig. 4. Discoloration of the UV-cured films during the accelerated weathering.

films during the accelerated weathering. As shown in Fig. 4, the discoloration increased with increasing exposure time. In particular, in the case of most the UV-cured films, the discoloration increased sharply up to ca. 384 h during the accelerated weathering. In the analysis of the measurement results, it was found that the UV-cured film containing the aromatic urethane linkage was particularly susceptible to discoloration, due to its poor ultraviolet resistance [12,13].

During the weathering of organic polymer materials, the lowest electron excitation energy is associated with the $\pi \rightarrow \pi^*$ transition involving the C═C, C═O and C═N bonds. These materials absorb strongly in the near ultraviolet region and are known as chromophores, which are the essential components of coloured compounds. Most organic bonds do not absorb UV light at frequencies above approximately 280 nm, and therefore are not directly damaged by sunlight. However, most resins used in coatings contain small amounts of peroxide and ketone impurities, which can absorb the sunlight to form free radicals, which initiate the process of photo-oxidation [14].

One important coating type which shows significant absorption of UV light at wavelengths above 280 nm is that composed of aromatic urethanes. Therefore, sunlight can directly break the bonds in this coating. In addition, urethane coatings made from aromatic precursors yellow badly in sunlight.

In UV-cured films containing the acrylated aromatic urethane oligomer, the UV-cured films, which were stabilized using stabilizers, showed a smaller colour difference than those not stabilized using light stabilizers. In this study, the colour difference of the UV-cured film, which was stabilized using both HALS and UVA, was the smallest. This study showed that HALS can protect UVA against the attack of free radicals, via the so-called synergistic effect of HALS [13].

In the case of the UV-cured film which was stabilized using UVA, UV light is absorbed by UVA. The absorbed radiative energy is converted mainly to heat by UVA, and then dissipated harmlessly. In the case of the 2-hydroxybenzotriazole-type ultraviolet light absorber (Tinuvin 384-2), the hydroxyl group allows energy to be absorbed by the molecule and dissipates this energy by a molecular rearrangement known as 'Keto-Enol tautomerism', as shown in Fig. 5 [14,15]. During the accelerated weathering, UVA (Tinuvin 384-2) absorbed more of the harmful light than HALS (Tinuvin 292), as shown in Fig. 6. Therefore, in the case of the UV-cured film which was stabilized using only HALS, the inhibitory action of HALS against the photodiscoloration was weak during the accelerated weathering.

UVA is helpful in inhibiting the photodiscoloration of the UV-cured film, due to its absorption of the harmful ultraviolet light, while HALS is not really helpful in inhibiting the photodiscoloration of the UV-cured film [13]. This is probably associated with the inability of HALS to trap the radicals produced by the photodiscoloration of the aromatic urethane resins.

The UV-cured film, which was stabilized using TiO_2, showed greater effectiveness than that stabilized using the light stabilizers (HALS or/and UVA) during the accelerated weathering. One of the primary motives for using pigments in coatings lies in their ability to protect the light-sensitive substrates and binders from UV attack, by selectively reflecting, scattering or absorbing all or a high percentage of the UV radiation [16].

In this study, during the accelerated weathering, the extent of discoloration of the UV-cured films was in the following order: Ar > ArH > ArU > Al/Ar ≥ ArUH ≥ ArP > Al.

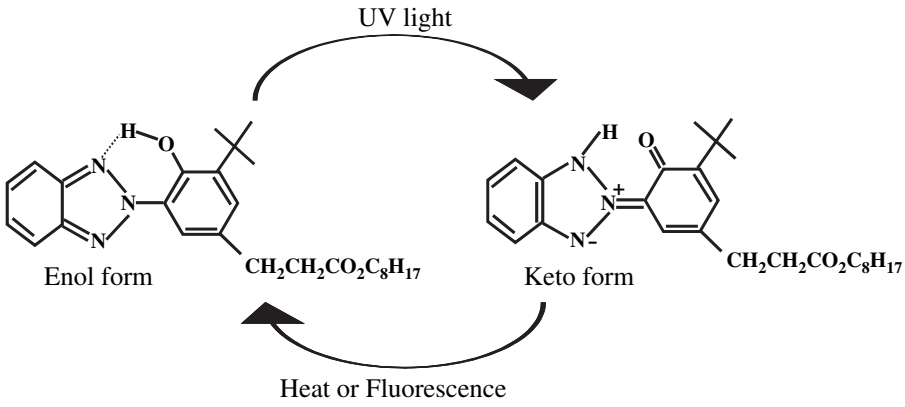

Fig. 5. Stabilizing mechanism of 2-hydroxybenzotriazole-type UV stabilizer.

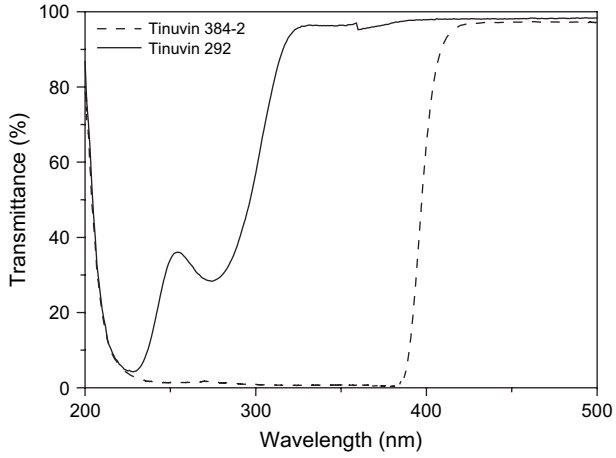

Fig. 6. UV/vis transmittance spectra of the light stabilizers (0.1% in acetonitrile).

3.2. Gloss

As shown in Fig. 7, the loss of gloss increased with increasing exposure time. In particular, in the case of the pigmented UV-cured film, the loss of gloss increased sharply during the accelerated weathering, although its discoloration was the smallest.

TiO_2 is the most widely used white pigment, particularly for exterior coatings. It has a high refractive index, which means that it has excellent hiding strength, and also provides a measure of protection against the harmful ultraviolet rays of sunlight, which can degrade many coating binders [14]. However, in this study, the loss of gloss in the UV-cured film containing the pigment was the highest. On the other hand, the loss of gloss in the UV-cured film, which was stabilized using both HALS and UVA, was the slightest.

In the case of the UV-cured film, which was stabilized using only HALS (or UVA), the improvement effect of the gloss retention was weak during the accelerated weathering. In this study, during the accelerated weathering, the extent of gloss retention of the UV-cured films was in the following order: ArUH > Al ≥ Al/Ar > ArU ≥ ArH > Ar > ArP.

The surface microstructure of clearcoats free from aromatics was found to increase considerably less than that of those with a higher aromatics content [17]. This provides evidence of the fact that the higher the concentration of aromatics, the more low-molecular weight products will be formed during the weathering process.

In addition, the increase in the microstructure involves an increase in the light diffusion, which in turn lowers the loss of gloss during weathering.

3.3. Hardness

Fig. 8 shows the influence of the isocyanate type of acrylated urethane oligomer, and that of the additives used, on the pendulum hardness of the UV-cured films before and after 960 h of exposure. The pendulum hardness of the UV-cured films increased with increasing exposure time [18–20].

During the UV exposure, the cured film becomes harder and loses most of its rubbery properties. As a consequence, the stress increases, especially at the surface of the cured film [18,20]. The photooxidation-induced damage causes changes in the chemical composition, as well as the crosslinking of the cured film during the weathering [18]. This, in turn, leads to the embrittlement of the cured film.

In addition, it is thought that the gradient associated with the change in chemical composition of the cured film is due to the presence of UVA in the cured film. As weathering progresses, the cured film embrittles and the amount of stress increases. Therefore, the brittleness and stress of the cured films lead to cracking, channeling and delamination [21]. In this study, after 960 h of accelerated weathering, the UV-cured film stabilized using both UVA and HALS gave the best results along with the lowest hardness.

Fig. 9 shows the difference in the loading/unloading curve of the UV-cured films before and after 960 h of accelerated weathering. As shown in Fig. 9, the higher the hardness, the higher is the resistance to plastic deformation. As expected,

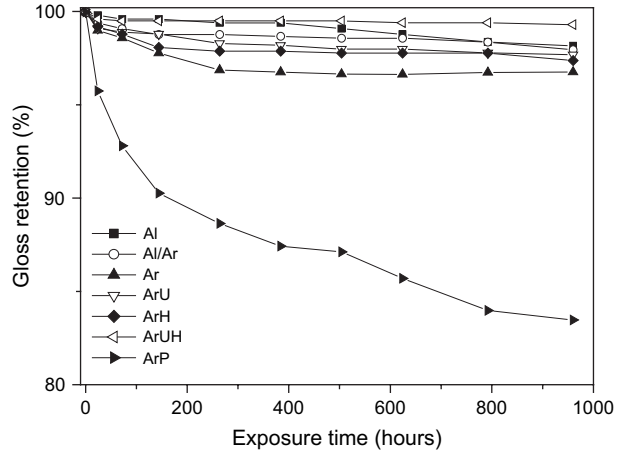

Fig. 7. Gloss of the UV-cured films during the accelerated weathering.

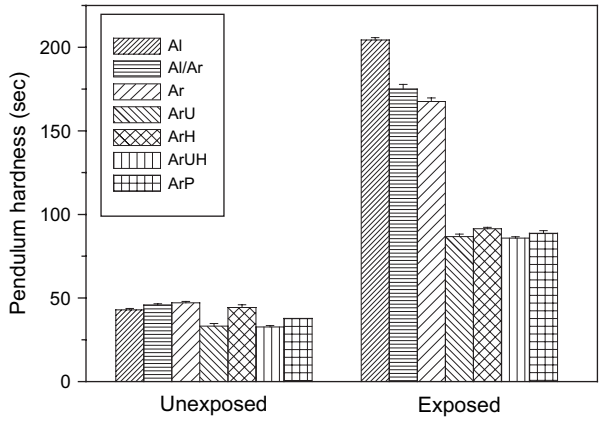

Fig. 8. Pendulum hardness of the UV-cured films before and after 960 h of accelerated weathering.

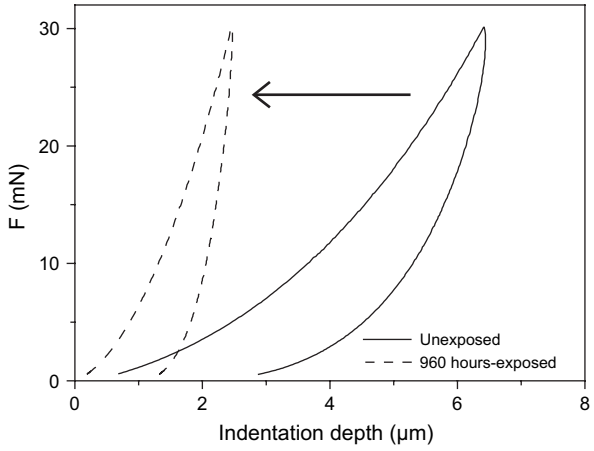

(a) Al

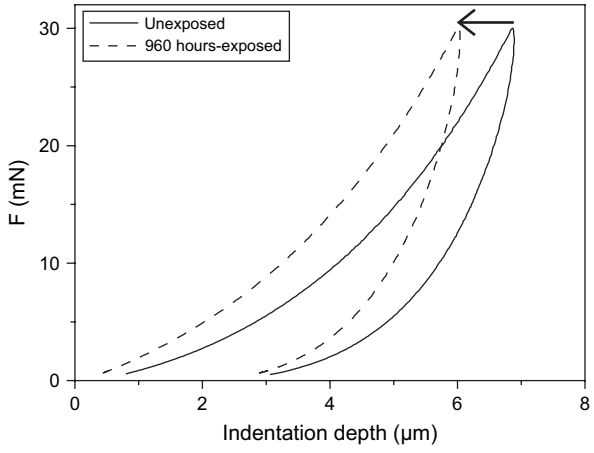

(b) ArUH

Fig. 9. Change in the loading/unloading curve of the UV-cured films before and after 960 h of accelerated weathering.

the area between the loading and unloading curve (plastic deformation) and maximum depth, d_{max}, of the diamond indenter penetration into the cured film decreased with increasing hardness of the cured film. As previously explained, the higher the hardness, the higher is the stress in the film during the accelerated weathering.

Fig. 10 shows the influence of the additives on the loading/unloading curve of the UV-cured films after 960 h of exposure. In the case of the UV-cured films containing the acrylated aromatic urethane oligomer, after 960 h of exposure, the hardness values were in the following order: Ar > ArP > ArH > ArU > ArUH. The highest hardness value observed for Ar is thought to be primarily due to the development of the highest stress in this UV-cured film.

As shown in Fig. 11, the elastic portion of the indentation work of the UV-cured films decreased with increasing exposure time. This result is associated with the decreased elastic recovery. However, the plastic portion of the indentation work increased. The loss in the elastic recovery of the polymer during weathering is associated with the chain degradation of the polymer as a function of exposure time [22]. The elastic

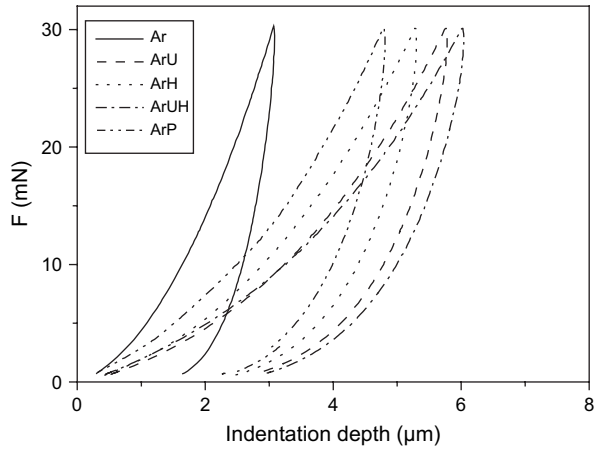

Fig. 10. Influence of additives on the loading/unloading curve of the UV-cured films after 960 h of accelerated weathering.

portion of the indentation work of the UV-cured films depended on the isocyanate type of the acrylated urethane oligomer used. The UV-cured film containing the acrylated aliphatic urethane oligomer had a higher elastic portion of

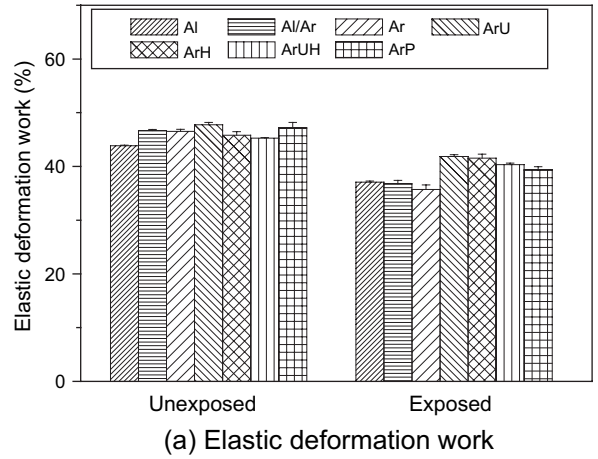

(a) Elastic deformation work

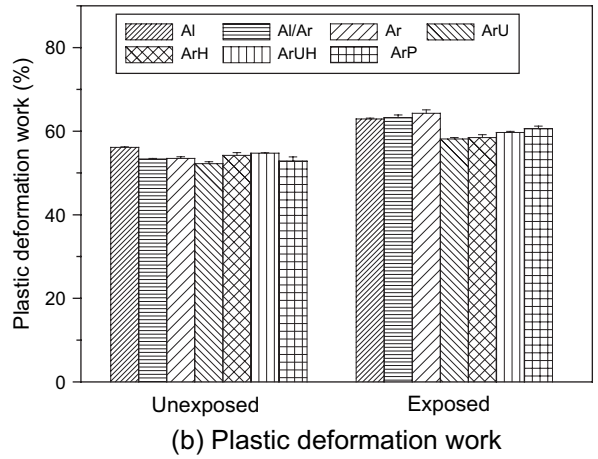

(b) Plastic deformation work

Fig. 11. Elastic deformation work and plastic deformation work of the UV-cured films before and after 960 h of accelerated weathering.

indentation work than that containing the acrylated aromatic urethane oligomer.

Fig. 12 shows the influence of the isocyanate type of acrylated urethane oligomer, and the additives, on the plastic hardness and universal hardness of the UV-cured films before and after 960 h of exposure. The value of the plastic hardness was higher than that of the universal hardness.

The universal hardness can be calculated from the maximum force, F_{max}, and the maximum penetration depth, h_{max}, which are related to both the plastic deformation and elastic deformation of the UV-cured film. However, the value of the plastic hardness can be calculated from the maximum force, F_{max}, and indenter penetration depth, h_{corr}, which are related solely to the plastic deformation of the UV-cured film.

As shown in Fig. 12, the addition of the additives decreased both the plastic hardness and universal hardness of the weathered UV-cured film. As a consequence, these additives were considered to be the main factors involved in the decrease in stress in the UV-cured film observed during the accelerated weathering.

As shown in Fig. 13, after 960 h of exposure, the elastic modulus of the UV-cured films increased. It was elucidated that the higher photodegradation resistance observed after the accelerated weathering, in the series of UV-cured films containing the aromatic and/or aliphatic isocyanate urethane oligomer not stabilized using additives, corresponds to their higher elastic portion of deformation indentation work, higher hardness, and higher elastic modulus.

However, the higher photodegradation resistance of the UV-cured aromatic urethane acrylate films, which were stabilized using various additives, corresponds to their higher plastic portion of deformation indentation work, lower hardness, and lower elastic modulus.

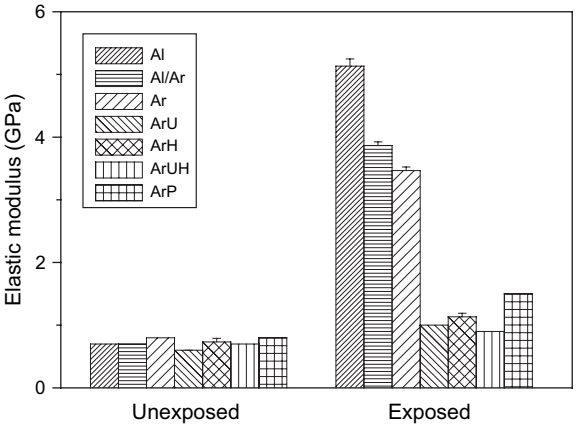

Fig. 13. Elastic modulus of the UV-cured films before and after 960 h of accelerated weathering.

3.4. FT-IR

Fig. 14 shows the IR spectra of the UV-cured films containing the acrylated aliphatic urethane oligomer, before and after exposure. As shown in Fig. 14, the size of the peak of the C–N stretch at around 1529 cm^{-1}, which is related to the urethane linkage, and the C–H stretch at around 2931 cm^{-1}, decreased with increasing exposure time [6,11,23].

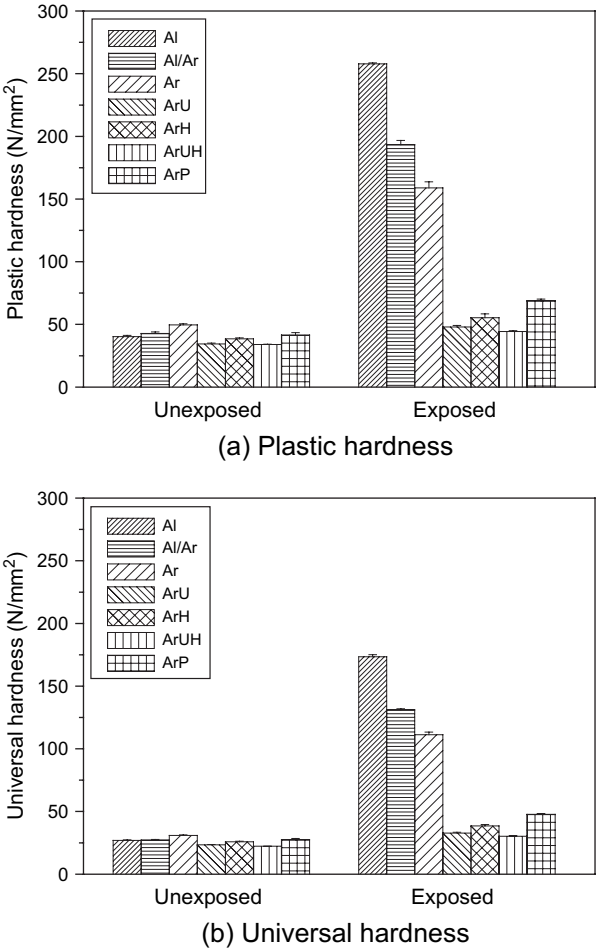

Fig. 12. Plastic hardness and universal hardness of the UV-cured films before and after 960 h of accelerated weathering.

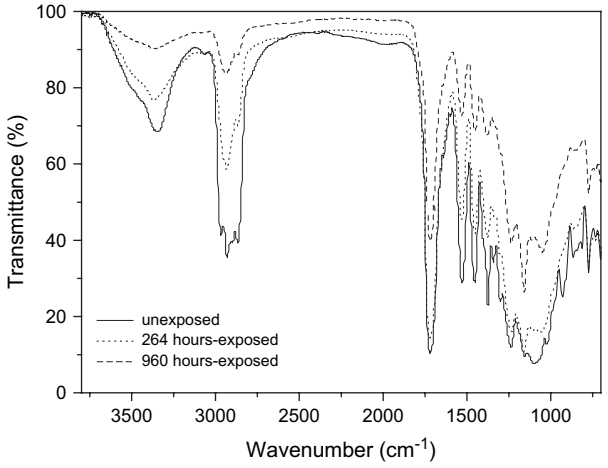

Fig. 14. IR spectra of the UV-cured films containing the acrylated aliphatic urethane oligomer before and after the accelerated weathering.

Fig. 15 shows the IR spectra of the UV-cured films containing the acrylated aromatic urethane oligomer with and without the light stabilizers (HALS and/or UVA). As shown in Fig. 15, during the accelerated weathering, the UV-cured films, which were stabilized using light stabilizers, showed a smaller decrease in the sizes of the peaks for the C–N stretch at around 1533 cm^{-1} (urethane linkage) and the C–H stretch at around 2931 cm^{-1} than was observed for the cured films which were not stabilized using light stabilizers.

The photodegradation of the UV-cured film containing the acrylated aromatic urethane oligomer was reduced by the addition of light stabilizers, as illustrated in Fig. 15. In particular, the UV-cured film, which was stabilized using both HALS and UVA, showed the smallest decrease in the size of the IR peaks for the C–N and C–H stretches.

During the accelerated weathering, the degree of photodegradation of the UV-cured films containing the acrylate aromatic oligomer was in the following order: Ar > ArH ≥ ArU > ArUH.

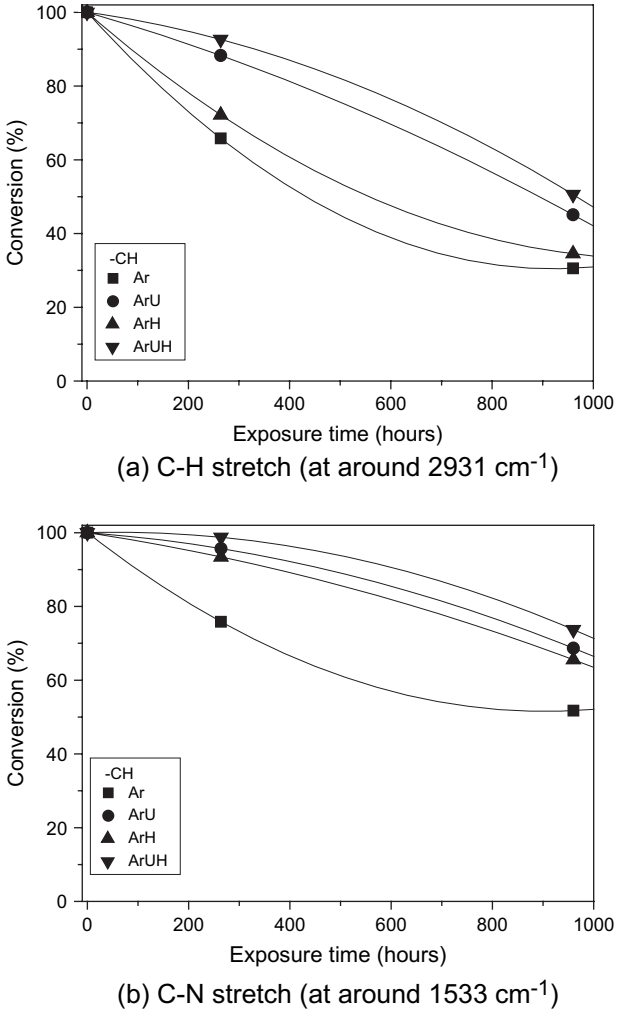

Fig. 15. Influence of the additives (HALS and UVA) on the UV-cured films containing the acrylated aromatic urethane oligomer during the accelerated weathering.

3.5. AFM

Fig. 16 shows the change in the surface morphology of the UV-cured films during the accelerated weathering. As shown in Fig. 16, after 960 h of exposure, the extent of degradation of the surface of the UV-cured films increased.

As previously explained in this study, the absorption of UV light by the impurities in the polymer backbone results in primary photochemical reactions, which in turn lead to photooxidative degradation of the polymer during the accelerated weathering [6,24]. As a consequence, the surface degradation of the cured films increases, as the weathering progresses [17].

Fig. 17 shows the influence of the additives (light stabilizer and pigment) on the surface morphology during the accelerated weathering. Fig. 17 shows the root mean square (RMS) roughness of the surface observed by AFM. As shown in Figs. 16 and 17, the surface roughness of the UV-cured films containing the acrylated aromatic oligomer increased with increasing exposure time. In particular, the UV-cured film, which was stabilized using light stabilizers, exhibited a smaller change in surface morphology than the one which was not stabilized using light stabilizers. However, although the UV-cured film containing the TiO_2 pigment showed high discoloration resistance, it also showed the highest surface roughness and gloss change. The gloss loss of the coating may be caused by the exposure of the TiO_2 on the surface of the UV-cured film during the accelerated weathering. As a consequence, the addition of the additives and the smaller aromatic concentration improved the photodegradation resistance of the cured film during the accelerated weathering.

4. Conclusions

The purpose of this study was to investigate the influence of the isocyanate type of acrylated urethane oligomer, and that of the additives (HALS, UVA and TiO_2) used, on the weathering of UV-cured films.

In the case of most of the UV-cured films, the discoloration increased sharply up to approximately 384 h during the accelerated weathering. The UV-cured film containing the acrylated aromatic urethane oligomer was more discoloured than that containing the acrylated aliphatic urethane oligomer. In particular, the discoloration of the UV-cured film, which was stabilized using both HALS and UVA, was the smallest.

In this study, the TiO_2 pigment was more effective at preventing the discoloration than the light stabilizers (HALS and UVA) during the accelerated weathering.

In the case of the gloss test, all of the UV-cured films showed high gloss retention (>95%) during the accelerated weathering. Although the UV-cured film containing the TiO_2 pigment exhibited the highest discoloration resistance, it nevertheless showed the highest gloss change. In the case of the UV-cured films containing the acrylated aromatic urethane oligomer, those containing the light stabilizers showed higher gloss retention than those without. The gloss retention of the UV-cured film, which was stabilized using both HALS and UVA, was the highest.

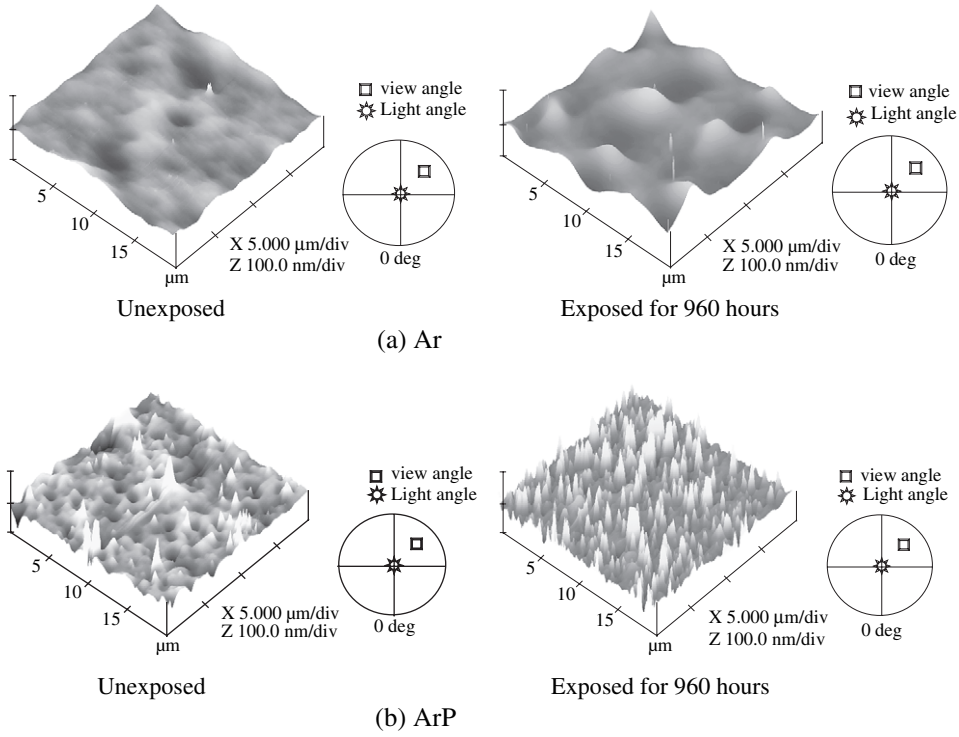

Fig. 16. AFM morphology change of the UV-cured films after 960 h of accelerated weathering.

In the case of the hardness test, the hardness and elastic modulus of all of the UV-cured films increased with increasing exposure time. In the case of the UV-cured films containing the acrylated aromatic urethane oligomer, after 960 h of exposure, those which contained one or more stabilizing additives (HALS, UVA and/or TiO_2), showed lower harnesses than those without. The UV-cured film, which was stabilized using both HALS and UVA, showed the lowest hardness, owing to the decrease in the stress in the UV-cured film. After 960 h of exposure, the elastic recovery of the deformed UV-cured films decreased. This decrease in the elastic recovery is associated with the increase in the plastic hardness.

As weathering progresses, the cured film embrittles and the amount of stress increases. Sometimes, the brittleness and stress of cured films may lead to cracking, channeling and delamination.

In addition, the FT-IR results showed that the degradation of the UV-cured films is related to the C–H stretch, and to the C–N stretch which is associated with the urethane linkage. These peaks decreased with increasing exposure time. In the case of the UV-cured films containing the acrylated aromatic urethane oligomer, those containing the light stabilizers showed a smaller decrease in the size of the C–N stretch peak than those without. The UV-cured film, which was stabilized using both HALS and UVA, showed the smallest decrease. This coincides with the other measurement results.

In the AFM analysis, the surface roughness of the UV-cured film increased with increasing exposure time. Those UV-cured films containing light stabilizers were more photostable than those without. The gloss retention of the UV-cured film, which was stabilized using both HALS and UVA, was the highest.

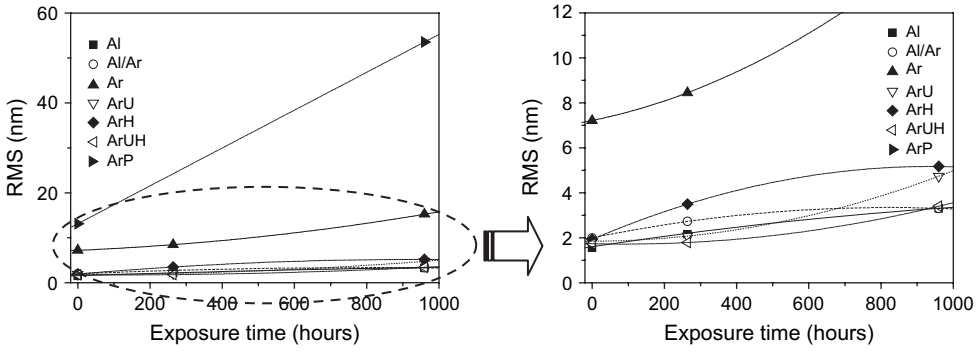

Fig. 17. Influence of the isocyanate type of acrylated urethane oligomer, and that of the additives (HALS, UVA and TiO_2) used, on the surface roughness of the UV-cured films during the accelerated weathering.

References

[1] Mehnert R, Pincus A, Janorsky I, Stowe R, Berejka A, editors. UV & EB curing technology & equipment. London: SITA Technology Ltd, John Wiley & Sons; 1998. p. 1–247.

[2] Seubert CM, Nichols ME, Cooper VA, Gerlock JL. The long-term weathering behavior of UV-curable clearcoats-I. Bulk chemical and physical analysis. Polymer Degradation and Stability 2003;81:103–15.

[3] Yang XF, Vang C, Tallman DE, Bierwagen GP, Croll SG, Rohlik S. Weathering degradation of a polyurethane coating. Polymer Degradation and Stability 2001;74:341–51.

[4] Singh RP, Tomer NS, Bhadraiah SV. Photo-oxidation studies on polyurethane coating: effect of additives on yellowing of polyurethane. Polymer Degradation and Stability 2001;73:443–6.

[5] Decker C. Specialty polymer additives – principles and applications: photostabilization of UV-curable coatings and thermosets. In: Al-Malaika S, Golovoy A, Wilkie CA, editors. UK: Blackwell Science Ltd; 2001. p. 139.

[6] Valet A. Outdoor applications of UV-curable clearcoats: a real alternative to thermally cured clearcoats. Progress in Organic Coatings 1999; 35:223–33.

[7] Ávár L, Bechtold K. Studies on the interaction of photoreactive light stabilizers and UV-absorbers. Progress in Organic Coatings 1999;35:11–7.

[8] ASTM D 4366. Standard test method for hardness of organic coating by pendulum damping tests; 1995.

[9] Musil J, Kunc F, Zeman H, Poláková H. Relationships between hardness, Young's modulus and elastic recovery in hard nanocomposite coatings. Surface and Coatings Technology 2000;154:304–13.

[10] Chang ST, Chou PL. Photo-discoloration of UV-curable acrylic coatings and the underlying wood. Polymer Degradation and Stability 1999; 63:435–9.

[11] Decker C, Zahouily K. Photostabilization of polymeric materials by photoset acrylate coatings. Radiation Physics and Chemistry 2002; 63:3–8.

[12] Wieczorrek W, Lohes F, Gempeler H, Schneider W, Neffgen B, Scherzer W. In: Stoye D, Freitag W, editors. Resins for coatings: chemistry, properties and applications. Polyadducts. Cinicinnati: Hanser/Gardner Publications, Inc; 1996. p. 177–221.

[13] Chang ST, Chou PL. Photodiscoloration inhibition of wood coated with UV-curable acrylic clear coatings and its elucidation. Polymer Degradation and Stability 2000;69:355–60.

[14] Weldon DG. Failure analysis of paints and coatings. New York: John Wiley & Sons; 2001. p. 1–29.

[15] Lee RE, Neri C, Malatesta V, Riva RM, Angaroni M. Specialty polymer additives: principles and applications. A new family of benzotriazoles: how to modulate properties within the same technology. In: Al-Malaika S, Golovoy A, Wilkie CA, editors. London: Blackwell Science Ltd; 2001. p. 119–38.

[16] Hare CM. Paint film degradation: mechanisms and control. Photolytically induced degradation-effect of pigment. In: Brady RF, editor. Pittsburgh, Pennsylvania: The Society for Protective Coatings; 2001. p. 337–62.

[17] Osterhold M, Glöckner P. Influence of weathering on physical properties of clearcoats. Progress in Organic Coatings 2001;41:177–82.

[18] Gregorovich BV, Adamsons K, Lin L. Scratch and mar and other mechanical properties as a function of chemical structure for automotive refinish coatings. Progress in Organic Coatings 2001;43:175–87.

[19] Irigoyen M, Bartolomeo P, Perrin FX, Aragon E, Vernet JL. UV ageing characterization of organic anticorrosion coatings by dynamic mechanical analysis, Vickers microhardness, and infra-red analysis. Polymer Degradation and Stability 2001;74:59–67.

[20] Bartolomeo P, Irigoyen M, Aragon E, Frizzi MA, Perrin FX. Dynamic mechanical analysis and Vickers microhardness correlation for polymer coating UV ageing characterization. Polymer Degradation and Stability 2001;72:63–8.

[21] Nichols ME, Gerlock JL, Smith CA, Darr CA. The effects of weathering on the mechanical performance of automotive paint systems. Progress in Organic Coatings 1999;35:153–9.

[22] Chew MYL, Goh SH, Kang LH, Tan N. Applicability of infrared spectroscopy for sealant degradation studies. Building and Environment 1999;34:49–55.

[23] Decker C, Zahouily K. Photodegradation and photooxidation of thermoset and UV-cured acrylate polymers. Polymer Degradation and Stability 1999;64:293–304.

[24] Schirmann PJ, Dexter M. Handbook of coatings additives: light and heat stabilizers for coatings. In: Calbo LJ, editor. New York: Marcel Dekker, Inc; 1987. p. 225–69.